

# PROCEEDINGS OF SPIE

[SPIDigitalLibrary.org/conference-proceedings-of-spie](https://spiedigitallibrary.org/conference-proceedings-of-spie)

## Fabrication of large-area twisted bilayer graphene for high-speed ultra-sensitive tunable photodetectors

Jiming Bao, Sirui Xing, Yanan Wang, Wei Wu, Francisco Robles-Hernandez, et al.

Jiming Bao, Sirui Xing, Yanan Wang, Wei Wu, Francisco Robles-Hernandez, Shin-shem Pei, "Fabrication of large-area twisted bilayer graphene for high-speed ultra-sensitive tunable photodetectors", Proc. SPIE 8725, Micro- and Nanotechnology Sensors, Systems, and Applications V, 872503 (29 May 2013); doi: 10.1117/12.2016049

**SPIE.**

Event: SPIE Defense, Security, and Sensing, 2013, Baltimore, Maryland, United States

# Fabrication of large-area twisted bilayer graphene for high-speed ultra-sensitive tunable photodetectors

Jiming Bao<sup>\*a</sup>, Sirui Xing<sup>a,b</sup>, Yanan Wang<sup>a</sup>, Wei Wu<sup>a,b</sup>, Francisco Robles-Hernandez<sup>c</sup>, Shin-shem Pei<sup>a,b</sup>

<sup>a</sup>Department of Electrical and Computer Engineering, University of Houston, Houston, TX 77204, USA; <sup>b</sup>Center for Advanced Materials, University of Houston, Houston, TX 77204, USA; <sup>c</sup>College of Engineering Technology, University of Houston, Houston, TX 77204, USA

## ABSTRACT

Single layer graphene has shown promising applications in fast and sensitive optoelectronic applications such as optical modulators and photodetectors. Twisted bilayer graphene has the potential to further improve the performances of such graphene devices due to its modified electronic band structure. However, the lack of synthesis method for large-area isolated twisted bilayer graphene has limited device applications. After a brief review of recent development in single layer graphene optoelectronic property and photodetectors, we discuss unique optical properties of twisted bilayer graphene. We then show two methods that we have developed to fabricate large-size twisted bilayer graphene islands. The first method uses chemical vapor deposition; the other method utilizes mechanical stacking of two large-size single-layer graphene hexagons. The realization of such twisted bilayer graphene samples enables new development of novel graphene-based devices.

**Keywords:** twisted bilayer graphene, Raman, enhanced absorption, photodetectors

## 1. INTRODUCTION

### 1.1 Graphene as an ideal optoelectronic material

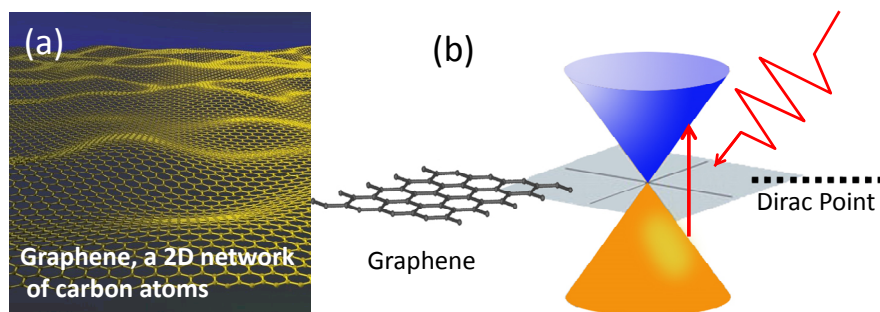


Figure 1. (a) Artist's illustration of a free-standing single-layer graphene. (b) Dirac cone-like electronic band structure and the absorption of a photon by graphene.

Graphene, a 2D network of carbon atoms (Fig. 1a), has attracted global interest because of its many unique properties. Graphene is also regarded as an excellent optoelectronic material owing to its high carrier mobility and a large optical response [1]. Its high electron mobility ( $> 200,000 \text{ cm}^2 \text{ V}^{-1} \text{ s}^{-1}$ ) and high saturation velocity of  $\sim 5 \times 10^7 \text{ cm s}^{-1}$  enables high-speed electronics [2-4]. As a comparison, the electron mobility of silicon is only  $\sim 1000 \text{ cm}^2 \text{ V}^{-1} \text{ s}^{-1}$ . Graphene also shows a strong and broadband optical response with 2% absorbance per layer over a broad spectrum [5, 6]. This absorption coefficient is orders of magnitude higher than those technologically important semiconductors such as

InGaAs, GaAs and germanium [5]. Both the high mobility and strong optical response are a result of its Dirac cone-like band structure shown in Fig. 1b. Because of these favorite optoelectronic properties, graphene has been used to demonstrate broadband photodetectors and optical modulators [7, 8].

### 1.2 Tunable optical absorption of graphene

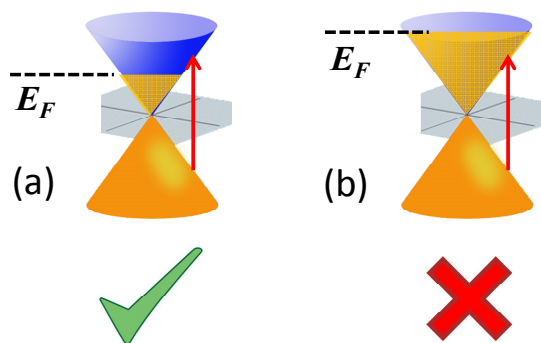


Figure 2. Modulation of optical absorption via the tuning of Fermi level. (a) Optical absorption is allowed when the final electronic state is empty. (b) Optical absorption is blocked when the final state is filled by electrons.

Graphene also offers another unique property that conventional semiconductors don't have: its optical response can be tuned over a large magnitude at a very fast speed [8]. Fig. 2 shows the principle of the modulation of optical absorption by tuning the Fermi level, which can be controlled by electrical gating. The absorption of a photon will create a pair of electron and hole. If the final state of the electron is filled by raising the Fermi level, then the electronic transition is not allowed, and the graphene becomes transparent at that wavelength. Such tunable optical response has been successfully employed to modulate the transmission of light through a silicon waveguide [8, 9]. A high modulation speed and a large modulation depth have been achieved.

### 1.3 Enhanced optical absorption in twisted bilayer graphene

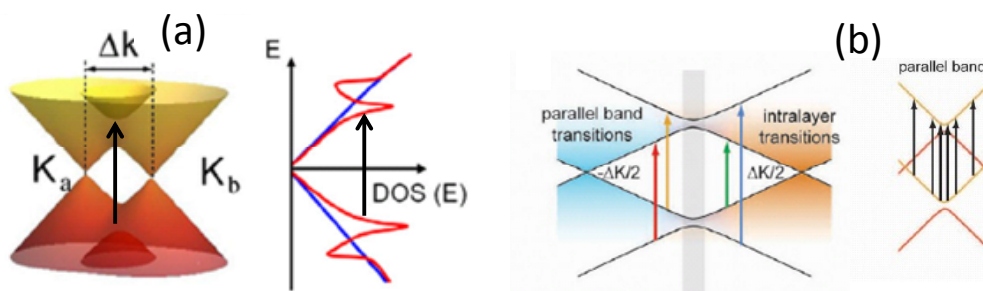


Figure 3. Electronic band structure of twisted bilayer graphene and its enhanced optical absorption. (a) Enhanced absorption due to large density of state (DOS) associated with Van Hove singularity at the intersection of two Dirac cones [10]. (b) Additional contribution to the enhanced absorption comes from parallel bands of two twisted graphene [11].

Although single layer graphene has a relatively strong optical response compared with other semiconductor thin films, a single layer graphene only absorbs ~2% of incident light. Increasing number of graphene layer will increase the optical absorption, but the mobility of electron will be reduced. For example, conventional bilayer graphene has a AB-stacking structure, its band structure becomes quite different from that of single layer graphene, The Dirac cone structure doesn't exist anymore, the band becomes parabolic at K point, similar to that of conventional semiconductor. This will significantly reduce mobility and saturation speed of electrons.

Significant increase in optical absorption can be realized in twisted bilayer graphene. Such enhanced optical absorption was manifested through the observation of G-line resonance, where the intensity of G-line Raman in twisted bilayer graphene (tBLG) increases by more than 30 fold compared with the G-line in single layer graphene at resonant wavelength[10-13]. This G-line resonance is due to the unique band structure of tBLG. As shown in Fig. 3, the band structure of tBLG can be approximated as a superposition of two rotated single-layer bands[10, 11]. The structure of Dirac cone is still preserved, which is why electrons in tBLG have single-layer like high electron mobility. The modification to the band structure happens at the intersection of two Dirac cones, where bands bend, leading to a high density of state (DOS), or Van Hove Singularity. Such enhanced DOS and parallel bands are responsible for the dramatically increased resonant optical absorption.

#### 1.4 Ultrafast graphene photodetectors

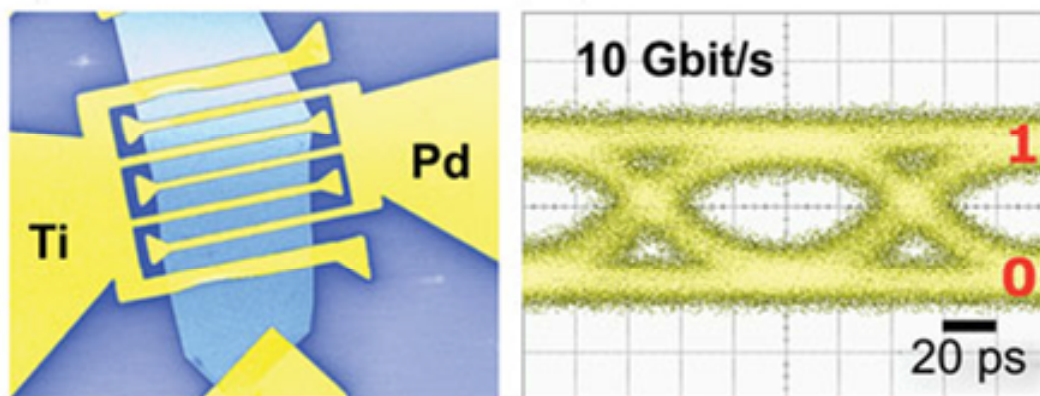


Figure 4. Photodetector based on single layer graphene [14]. (a) Device structure of a graphene photodetector. (b) “Eye diagram” shows the 10 Gbit/s data rate by graphene photodetector.

Because of the favorite properties of graphene for optoelectronic devices, graphene photodetectors were first reported in 2009[14]. Fig. 4a shows a revised structure where finger structure and two metals with different work functions are used to enhance the photoresponse. As shown in Fig. 4b, such graphene photodetectors have demonstrated 10 Gbit/s data streaming rate[14].

Due to the limited optical absorption of single layer graphene (~2%), the overall photoresponse is still small compared with conventional detector based on semiconductors. In order to enhance the photoresponse, a number of novel device configurations have been proposed and demonstrated [15-17]. The first method is to utilize surface plasmon resonance of Au electrode[15]. An enhancement of 20 times was demonstrated. The other methods make use of enhanced field in a microcavity[16, 17]. In one case, the microcavity was made of dielectric Bragg reflectors[16]. In other case, high reflecting mirrors were used [17]. In all these cases, there is a strong requirement for the design of nanostructures.

## 2. Synthesis of large-size twisted bilayer graphene

### 2.1 Synthesis of single layer graphene

Single layer graphene was grown by chemical vapor deposition (CVD) using  $\text{CH}_4$  as the carbon feedstock on Cu substrates at ambient pressure [18-20]. A Cu foil (25- $\mu\text{m}$ -thick, 99.8%, Alfa Aesar) was first loaded into a CVD furnace and heated up to 1,050 °C under 300 s.c.c.m. Ar and 10 s.c.c.m.  $\text{H}_2$ . After reaching 1050 °C, the sample was annealed for

30 min or longer without changing the gas flow rates. The growth was then carried out at 1050 °C under a gas mixture of 300 s.c.c.m. diluted (in Ar) CH<sub>4</sub> (concentration 8 ppm) and 10 s.c.c.m. of H<sub>2</sub>. Finally, the sample was rapidly cooled to room temperature under the protection of Ar and H<sub>2</sub>, and taken out of the furnace for characterization. Graphene was transferred onto SiO<sub>2</sub>/Si wafers (doped Si covered by 300nm SiO<sub>2</sub>) using a PMMA (polymethyl methacrylate)-assisted process.

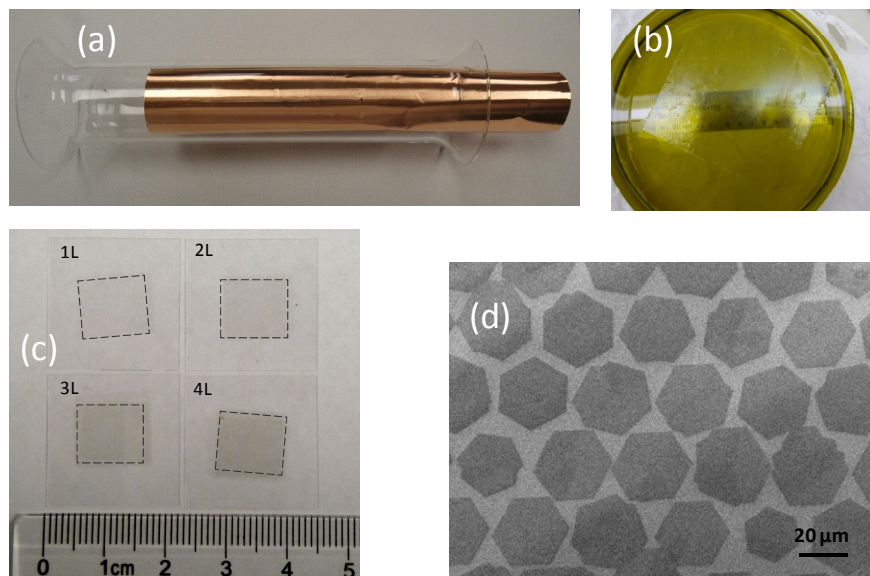


Figure 5. Graphene synthesis. (a) Copper foil for growth of large-area graphene using chemical vapor deposition (CVD). (b) A floating PMMA/graphene after etching of copper substrate by ferric nitrate. (c) Graphene transferred to glass substrates. Multilayer (2L-4L) graphene is obtained by stacking monolayer (1L) graphene. (d) Array of single-crystal monolayer graphene.

Fig. 5a shows a Cu foil loaded in a quartz tube for graphene CVD graphene synthesis. Graphene can grow on both sides of the foil. PMMA is spin coated on one side of the Cu foil, graphene on the other side is removed using reactive ion etching. To remove Cu substrate without causing damage to graphene/PMMA film, the Cu foil is then immersed in a ferric nitrate acid. After Cu foil is completely dissolved, the graphene/PMMA film begins to float on the acid surface as shown in Fig. 5b. The film can be scooped onto any substrate, with graphene left after removal of PMMA by acetone. Such PMMA-assisted graphene transfer can be repeated several times to create stacked multi-layer graphene as shown in Fig. 5c. When the growth time is longer than 30 minutes, a continuous single-layer graphene is obtained. Isolated graphene grains are obtained when the growth time is limited to 10 minutes [19]. By preparing arrays of seed carbon, arrays of graphene hexagons can be obtained as shown in Fig. 5d [19].

## 2.2 Synthesis and optical properties of twisted bilayer graphene

Twisted bilayer graphene (tBLG) has the potential to enhance optical response dramatically, but their current fabrication techniques limit their device applications because of their small size [10-12]. A well isolated tBLG with the size of at least a few micrometers is needed for basic device fabrication and characterization. Here we present two methods to fabricate such tBLG.

## 2.2a Twisted bilayer graphene by CVD synthesis

In order to synthesize isolated bilayer graphene islands, we increased  $\text{CH}_4$  flow and reduce synthesis time [13, 21, 22]. Fig. 5a shows an example of well isolated twisted bilayer graphene islands. Compared with previously reported tBLG, our tBLG samples have two desired properties: (1) each graphene layer has a hexagonal shape so that the twist angle can be directly obtained from electron or optical microscopy [22]. (2) Each graphene layer has a single domain, and the bilayer island is separated from other islands. Raman spectrum in Fig. 6b shows a distinctive G-line resonance under 532-nm laser excitation, in agreement with the rotation angle [13]. The associated G-line and 2D-band mappings in Fig. 6c-d further confirm the single domain nature of both graphene layers.

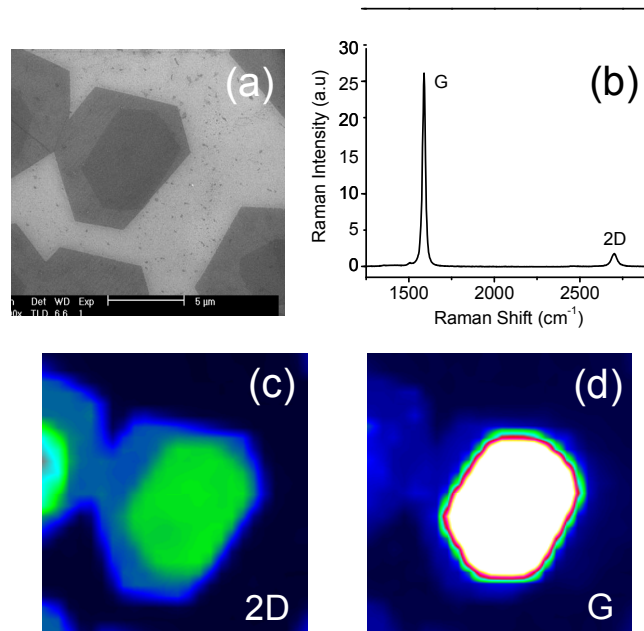


Figure 6. Characterizations of twisted bilayer graphene (tBLG) synthesized by CVD. (a) Scanning electron microscopy (SEM) picture of a representative tBLG hexagon with a  $\sim 13^\circ$  rotation angle. Scale bar: 5  $\mu\text{m}$ . (b) Its Raman spectrum illustrating the G-line resonance under 532-nm laser excitation. (c-d) Raman mappings of the graphene island. (c) 2D-band Raman mapping. (d) G-line Raman mapping

## 2.2b Twisted bilayer graphene by stacking two monolayer graphene

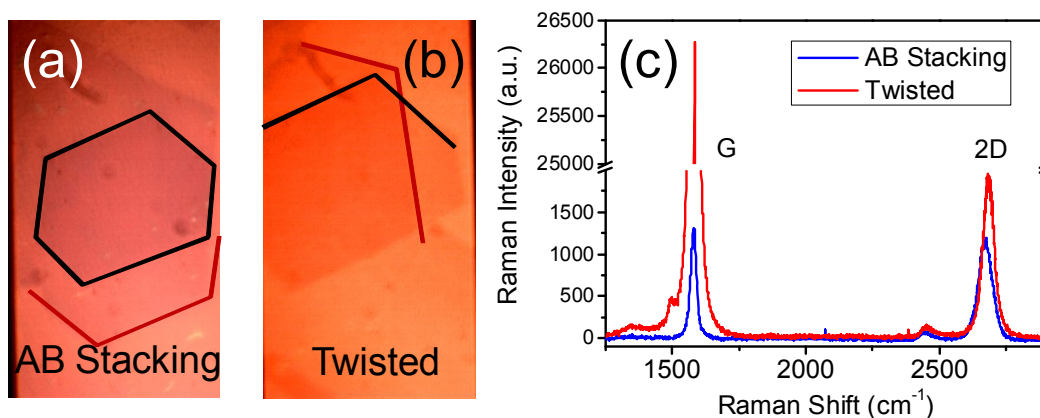


Figure 7. Bilayer graphene samples fabricated by stacking two large-size monolayer graphene islands. (a-b) AB stacking and twisted bilayer graphene islands. Lines indicate edges of single layer graphene islands. (c) Corresponding Raman spectra. The size of each graphene island is about 100  $\mu\text{m}$ .

Another method to fabricate isolated tBLG islands is to stack two monolayer graphene islands. It should be noted that large size monolayer graphene islands have to be prepared first. To achieve this, we reduced CH<sub>4</sub> flow rate while increasing growth time to 2 hours. Much larger single layer graphene hexagons are obtained with an average diameter of 100 μm. Fig. 7 a-b show two types of bilayer graphene islands: AB-stacking and twisted bilayer graphene. Raman spectra in Fig. 7c reveal the expected big difference between AB-stacking and twisted bilayer graphene in G-line and 2D-band Raman spectra.

### 3. CONCLUSIONS

We propose to use twisted bilayer graphene for developing new generation of graphene optoelectronic devices. We have demonstrated synthesis of large-size twisted graphene islands using two distinct methods: chemical vapor deposition and mechanical stacking of large-size monolayer graphene hexagons. Such isolated large-size twisted bilayer graphene materials will enable new graphene optoelectronic devices with a higher speed and an enhanced optical response.

### References

- [1] Avouris, P. and Xia, F.N., "Graphene applications in electronics and photonics," *Mrs Bulletin* 37, 1225-1234 (2012).
- [2] Bolotin, K.I., et al., "Ultrahigh electron mobility in suspended graphene," *Solid State Communications* 146, 351-355 (2008).
- [3] Du, X., et al., "Approaching ballistic transport in suspended graphene," *Nature Nanotechnology* 3, 491-495 (2008).
- [4] Schwierz, F., "Graphene transistors," *Nature Nanotechnology* 5, 487-496 (2010).
- [5] Nair, R.R., et al., "Fine structure constant defines visual transparency of graphene," *Science* 320, 1308-1308 (2008).
- [6] Kuzmenko, A.B., et al., "Universal optical conductance of graphite," *Physical Review Letters* 100, (2008).
- [7] Mueller, T., Xia, F.N.A., and Avouris, P., "Graphene photodetectors for high-speed optical communications," *Nature Photonics* 4, 297-301 (2010).
- [8] Liu, M., et al., "A graphene-based broadband optical modulator," *Nature* 474, 64-67 (2011).
- [9] Liu, M., Yin, X.B., and Zhang, X., "Double-Layer Graphene Optical Modulator," *Nano Letters* 12, 1482-1485 (2012).
- [10] Kim, K., et al., "Raman Spectroscopy Study of Rotated Double-Layer Graphene: Misorientation-Angle Dependence of Electronic Structure," *Physical Review Letters* 108, 246103 (2012).
- [11] Havener, R.W., et al., "Angle-Resolved Raman Imaging of Inter layer Rotations and Interactions in Twisted Bilayer Graphene," *Nano Letters* 12, 3162-3167 (2012).
- [12] Ni, Z.H., et al., "G-band Raman double resonance in twisted bilayer graphene: Evidence of band splitting and folding," *Physical Review B* 80, 125404 (2009).
- [13] Yanan Wang, et al., "Twisted Bilayer Graphene Superlattices," <http://arxiv.org/abs/1301.4488> (2013).
- [14] Xia, F.N., et al., "Ultrafast graphene photodetector," *Nature Nanotechnology* 4, 839-843 (2009).
- [15] Echtermeyer, T.J., et al., "Strong plasmonic enhancement of photovoltage in graphene," *Nature Communications* 2, (2011).
- [16] Furchi, M., et al., "Microcavity-Integrated Graphene Photodetector," *Nano Letters* 12, 2773-2777 (2012).
- [17] Engel, M., et al., "Light-matter interaction in a microcavity-controlled graphene transistor," *Nature Communications* 3, (2012).
- [18] Wu, W., et al., "Wafer-scale synthesis of graphene by chemical vapor deposition and its application in hydrogen sensing," *Sensors and Actuators B-Chemical* 150, 296-300 (2010).
- [19] Yu, Q.K., et al., "Control and characterization of individual grains and grain boundaries in graphene grown by chemical vapour deposition," *Nature Materials* 10, 443-449 (2011).
- [20] Yu, Q.K., et al., "Graphene segregated on Ni surfaces and transferred to insulators," *Applied Physics Letters* 93, 113103 (2008).
- [21] Wu, W., et al., "Control of thickness uniformity and grain size in graphene films for transparent conductive electrodes," *Nanotechnology* 23, (2012).
- [22] Nie, S., et al., "Growth from below: bilayer graphene on copper by chemical vapor deposition," *New Journal of Physics* 14, (2012).